ChemSusChem

Research Article
doi.org/10.1002/cssc.202301721

Chemistry Europe
European Chemical Societies Publishing

www.chemsuschem.org

Coupling of CO_2 Electrolysis with Parallel and Semi-Automated Biopolymer Synthesis – Ex-Cell and without Downstream Processing

Ida Dinges,[a, b] Ina Depentori,[a] Lisa Gans,[a] Dirk Holtmann,[c] Siegfried R. Waldvogel,[b, d] and Markus Stöckl*[a]

Important improvements have been achieved in developing the coupling of electrochemical CO_2 reduction to formate with its subsequent microbial conversion to polyhydroxybutyrate (PHB) by *Cupriavidus necator*. The CO_2 based formate electrosynthesis was optimised by electrolysis parameter adjustment and application of Sn based gas diffusion electrodes reaching almost 80% Faradaic efficiency at 150 mA cm^{-2}. Thereby, catholyte with the high formate concentration of 441 ± 9 mmol L^{-1} was generated as feedstock without intermediate downstream processing for semi-automated formate feeding into a fed-batch reactor system. Moreover, microbial formate conversion to PHB was studied further, optimised, and successfully scaled from shake flasks to semi-automated bioreactors. Therein, a PHB per formate ratio of 16.5 ± 4.0 mg g^{-1} and a PHB synthesis rate of 8.4 ± 2.1 mg L^{-1} OD^{-1} h^{-1} were achieved. By this process combination, an almost doubled overall process yield of 22.3 ± 5.5% was achieved compared to previous reports. The findings allow a detailed evaluation of the overall CO_2 to PHB conversion, providing the basis for potential technical exploitation.

Introduction

The contemporary global chemical industry relies upon fossil resources as energy source and feedstock for basic chemicals. However, the world's fossil resources are ultimately limited, and their use leads to high CO_2 emissions, accelerating the climate change. Consequently, the chemical industry needs to replace fossil resources with renewable energy sources and secure alternative access to basic chemicals. Thereby, the electrification of chemical processes will represent one of the main building blocks in the future.[1–3]

With this in mind, the electrochemical CO_2 reduction reaction (*eCO$_2$RR*) offers the promising opportunity to convert CO_2 into higher value chemicals using renewable electricity.[4,5] In general, the reduction of gaseous CO_2 at technically relevant current densities (> 100 mA cm^{-2},[6–8] strongly depended on the electrolysis product) requires gas diffusion electrodes (GDE),[9–11] as gaseous CO_2 has a low solubility in aqueous electrolytes (33 mmol L^{-1} at 298 K and 1 atm).[12,13] Besides the *eCO$_2$RR* to carbon monoxide,[14–16] the electrosynthesis of formic acid/formate represents a far developed reaction, which has been reported in numerous studies with outstanding performance indicators such as current density up to 1.8 A cm^{-2},[17] Faradaic efficiency (FE) above 90%,[9,18] long-time process stability of 1000 h[19] and high product concentration (20 wt% formic acid).[20]

Based on this tremendous scientific effort, formic acid/formate originating from *eCO$_2$RR* is considered to become economically viable in the near future.[7] However, it has to be pointed out that for a successful substitution of fossil feedstock, more complex and more reduced carbon based chemicals are demanded, and an upgrade, e.g. based on formate, is required. An elegant option to transform formate into more complex and higher value products is its use as substrate in biotechnological syntheses.[21–23] This kind of process combination is exemplarily illustrated in Figure 1 (Section 1).

Several organisms such as *Acetobacterium woodii*, *Eubacterium limosum* or *Methylobacterium extroquens* have been reported as possible biocatalysts for a formate based bioeconomy.[21,23] Within this study, the well-established formatotrophic model organism *Cupriavidus necator* (*C. necator*) was used, which has been shown to produce a variety of products, ranging from polyhydroxybutyrate[24,25] (PHB) in the wildtype

[a] I. Dinges, I. Depentori, L. Gans, Dr. M. Stöckl
Chemical Technology
DECHEMA Research Institute
Theodor-Heuss-Allee 25, 60486 Frankfurt am Main, Germany
E-mail: markus.stoeckl@dechema.de

[b] I. Dinges, Prof. Dr. S. R. Waldvogel
Department of Chemistry
Johannes Gutenberg University Mainz
Duesbergweg 10–14, 55128 Mainz, Germany

[c] Prof. Dr. Ing. D. Holtmann
Institute of Process Engineering in Life Sciences
Karlsruhe Institute of Technology
Fritz-Haber-Weg 4, 76131 Karlsruhe, Germany

[d] Prof. Dr. S. R. Waldvogel
Institute of Biological and Chemical, Systems – Functional Molecular Systems (IBCS-FMS)
Karlsruhe Institute of Technology
Kaiserstraße 12, 76131 Karlsruhe, Germany.

Supporting information for this article is available on the WWW under https://doi.org/10.1002/cssc.202301721

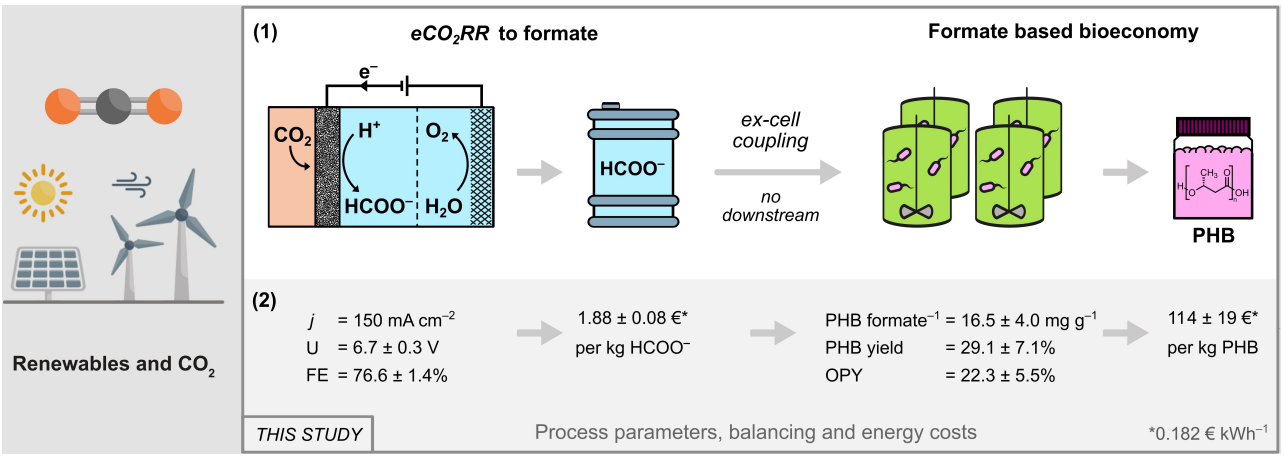

Figure 1. Schematic illustration of the overall process combination of the electrochemical CO_2 reduction reaction (*eCO₂RR*) to formate with a formate based bioeconomy using renewable energy sources. (1) Ex-cell coupling of *eCO₂RR* to formate with its subsequent microbial conversion to polyhydroxybutyrate (PHB) by *Cupriavidus necator* without intermediate downstream processing. (2) Key process data as well as resulting costs for formate and PHB based on a recent energy price[35] achieved in this study. Abbreviations: j = Current density, U = Average terminal voltage, FE = Faradaic efficiency for formate, OPY = Overall process yield.

strain to solvents,[26–29] organic acids[30,31] and terpenes[32,33] with genetically modified strains.

Even though the combination of the *eCO₂RR* and the subsequent biosynthesis of higher value products is a promising route to substitute fossil raw materials, the technical combination of the latter processes is challenging. In general, a suitable process combination can be realised by an "in-cell" or "ex-cell" coupling. In in-cell processes (or secondary microbial electrochemical technologies),[34] *eCO₂RR* to formate and its subsequent microbial conversion would take place in the same reactor (system), whereas an ex-cell coupling keeps both subprocesses separated in both space and time. To the authors' point of view, the ex-cell coupling of *eCO₂RR* and biosynthesis provides a variety of advantages, since it allows their process parameters to be optimised and operated more independently.

In previous work,[25] the initial coupling of *eCO₂RR* to formate with its subsequent microbial conversion to PHB by *C. necator* was demonstrated, but several challenges were not solved: Both subprocesses were kept spatially separated. Formate was electrochemically synthesised from CO_2 in a flow reactor with a Sn based GDE in 0.2 M KH_2PO_4/K_2HPO_4 as a biocompatible electrolyte. Back then, a FE for formate of 49.7 ± 0.9% at 50 mA cm^{-2} was achieved. The biocompatible catholyte containing electrosynthesised formate (e-formate) was used as substrate for microbial PHB synthesis with *C. necator* in shake flasks without intermediate downstream processing, leading to a final PHB concentration of 56 mg L^{-1} solely on e-formate and an overall FE of 4% for the coupled processes. Herein, very important challenges were solved by the improvement of individual subprocesses and harmonisation of the coupling based on previous findings, and an overall process was established and evaluated (Figure 1, Section 1 and 2).

Results and Discussion

The CO_2 based formate electrosynthesis (first subprocess) was mainly optimised by application of self-fabricated GDEs. Thereby, catholyte with high e-formate concentration was produced as feedstock for *C. necator*. Moreover, microbial formate conversion to PHB (second subprocess) was examined and successfully transferred as well as scaled from shake flasks to a fed-batch reactor system with a semi-automated e-formate feed. Three different phosphate buffers were examined for both subprocesses, they only differ in their K^+ and Na^+ contents. They were derived from the physiological, biocompatible 0.2 M phosphate buffer employed for the initial successful coupling. This is in turn an adaption of Sydow et al.,[36] who developed an electrolysis-compatible cultivation medium for *C. necator* based on phosphates. To avoid any intermediate downstream processing, all buffer compositions were examined for both subprocesses individually.

Gas Diffusion Electrodes

GDEs were fabricated by heat pressing the catalyst mixture onto support material. Sn powder of inexpensive origin (approx. 95 € kg^{-1}) with particle sizes ≤ 20 µm was used as electrocatalyst and polytetrafluoroethylene (PTFE) powder served as hydrophobic binder in the catalyst mixture. Both materials were homogenised and pressed onto Ni foam, which served as support material and current collector. Taking current prices into account, material cost of GDE fabrication was estimated at approx. 436 € m^{-2}, of which Ni foam accounts for 79%. In total, twelve GDEs were fabricated for the herein presented electrolyses using a relatively inexpensive electrocatalyst by a fast, easy, and scalable fabrication method. The reproducibility of this predominantly manual fabrication method was sufficient and no influence of the minor fabrication variation on GDE

performance was observed (Sn loading b (Sn, wt%) = 90 ± 4 mg cm^{-2} and thickness d = 558 ± 15 µm, n = 12). Further details and photographs are provided in the Supporting Information (SI, Section 1.2 and 3.2).

Formate Electrosynthesis

Electrochemical CO_2 reduction was carried out in a gas-fed flow reactor with three different phosphate-based electrolytes regarding microbial PHB synthesis optimisation: (A) 0.2 M KH_2PO_4/K_2HPO_4, (B) 0.2 M NaH_2PO_4/K_2HPO_4 and (C) 0.2 M NaH_2PO_4/Na_2HPO_4 (equimolar, respectively), with pH values of 6.67 ± 0.05 (A, n = 3), 6.61 ± 0.05 (B, n = 6) and 6.53 ± 0.05 (C, n = 3). To use formate-containing catholyte as feedstock in semi-automated bioreactors, the aim was to achieve the highest possible formate concentration at high FE produced with a high energy efficiency. For this purpose, all electrolyses were run for 22 h, maintaining current density at 150 mA cm^{-2} after an initial ramp (12.5 mA cm^{-2} increase every 5 min). Figure 2 compares FE and concentration of formate in the catholyte obtained during electrolysis for the different electrolytes.

Generally, all three FE courses showed a decrease during the 22 h runtime. This was accompanied by a deterioration of formate production rates between the first and second fitted intervals (Interval 1 = 1–6 h, interval 2 = 19–22 h). These deteriorations were attributed to presumed formate mass transport limitations within the GDE's pore system increasing the influence of the parasitic hydrogen evolution reaction (HER). This hypothesis was supported by gas chromatography (GC) analysis, as hydrogen was detected as sole byproduct for all electrolyses (SI, Section 1.8). Final formate FE's of 79.8 ± 1.3% (A, n = 3), 76.6 ± 1.4% (B, n = 6) and 63 ± 2% (C, n = 3) were achieved. These were accompanied by catholyte formate concentrations of 458 ± 7 mmol L^{-1} (A, n = 3), 441 ± 9 mmol L^{-1} (B, n = 6) and 358 ± 11 mmol L^{-1} (C, n = 3). Consequently, electrolysis results of electrolyte (A) and (B) were relatively similar, while those of (C) were significantly inferior. Furthermore, electrolyses with electrolyte (A) and (B) were more energy efficient compared to electrolyte (C). In electrolyte (A), electrolyses required an average terminal voltage (U) of 6.38 ± 0.15 V (n = 3) and consumed 104 ± 3 Wh (n = 3) of electric energy. Similarly, electrolyses with (B) were run at 6.7 ± 0.3 V (n = 6) with an electric energy consumption (EEC) of 110 ± 4 Wh (n = 6). In contrast, using electrolyte (C) resulted in 7.54 ± 0.14 V (n = 3) combined with an EEC of 123 ± 3 Wh (n = 3).

Taking everything into account, electrolyte (A) containing only K^+ as alkali cation yielded the best results among the examined electrolytes. Results for electrolyte (B) with Na^+/K^+ (1:2) were only slightly lower, whereas electrolyte (C) led to the lowest electrolysis performance of all three. It was hypothesised that the electrolytes decreasing conductivity from (A, 24.0 mS cm^{-1} at 23.4 °C) over (B, 21.8 mS cm^{-1} at 23.5 °C) to (C, 17.1 mS cm^{-1} at 23.4 °C) was responsible for this. Lower conductivity leads to a higher terminal voltage necessary to maintain the set current density, which resulted in a higher GDE potential favouring HER. Averaged for electrolysis duration and referenced to a reversible hydrogen electrode (RHE), the GDE potentials were −1.79 ± 0.14 V (A, n = 3), −1.74 ± 0.06 V (B, n = 6) and −1.86 ± 0.13 V (C, n = 3). Nonetheless, all electrolysis systems presented herein outperform the preceding study,[25] on which this study was based. Back then, only 49.7 ± 0.9% formate FE were achieved at 50 mA cm^{-2} employing electrolyte (A). This shows that the optimised Sn based GDEs with adjusted electrolysis conditions achieved an over 25% higher formate FE in the same electrolyte at tripled current density.

As mentioned in the introduction, higher FE (90%)[9] and higher current densities (1.8 A cm^{-2})[17] than those described here have already been published. However, the combination of the achieved FE of almost 80% at 150 mA cm^{-2} in 22 h of electrolysis with a final formate concentration around 450 mmol L^{-1} was achieved directly in a biocompatible electrolyte, which is suitable for the direct application as feed for the microbial PHB synthesis. Recently, Lim et al.[37] carried out a similar coupling, in which they reported slightly lower values of 66% FE for formate at 120 mA cm^{-2}.

Besides the herein improved FE and constant current density, the initial current density ramp of the electrolysis start-

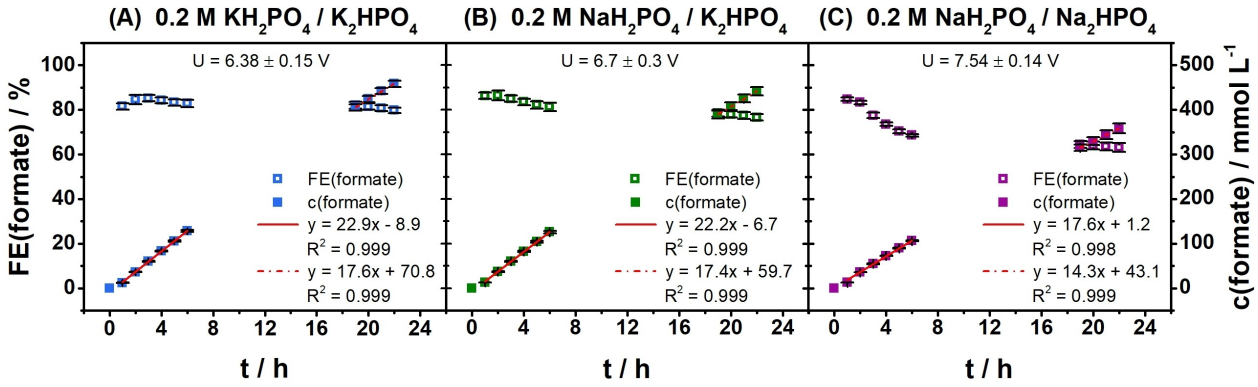

Figure 2. Faradaic efficiency (FE) and concentration course of formate in the catholyte of CO_2 electrolyses with different electrolytes: (A) 0.2 M KH_2PO_4/K_2HPO_4 (n = 3, blue), (B) 0.2 M NaH_2PO_4/K_2HPO_4 (n = 6, green) and (C) 0.2 M NaH_2PO_4/Na_2HPO_4 (n = 3, purple). Formate concentration courses were fitted linearly in two intervals: t = 1–6 h (red, solid line) and t = 19–22 h (red, dash dot line). Electrolysis parameters: Initial ramp (12.5 mA cm^{-2} increase every 5 min), Constant current density j = 150 mA cm^{-2} (after ramp), Runtime = 22 h (≙ 58162.5 C), Initial V (catholyte, anolyte) = 500 mL each, Cathode (GDE): 87.5% Sn, 12.5% PTFE on Ni foam, Reference electrode: Reversible hydrogen electrode (RHE), Anode: Mixed Ir-oxide on a Ti-grid (Platinode EP, Type 177, Umicore).

up procedure demonstrated that the GDE's performance was relatively stable at different current densities until at least the final 150 mA cm^{-2}. This is an advantage, as fluctuating electric energy originating from renewable sources could be compensated by adjusting current density of the electrolysis, which would be enabled by flexibly operable GDEs.

Catholyte Characterisation

After electrolysis, the three catholytes intended as e-formate feedstock were further characterised. On the one hand, their Sn^{2+} content was determined via inductively coupled plasma atomic emission spectroscopy (ICP-OES) to investigate cathodic corrosion[38] of the self-fabricated GDEs. On the other hand, the concentrations of Na^+, K^+ an PO_4^{3-} were determined by ion chromatography (IC) to examine possible differences compared to their initial concentrations. The cation analysis data of the catholyte characterisation are summarised in Table 1.

ICP-OES analysis showed that only traces of dissolved electrocatalyst were found in the catholyte for all three electrolytes after 22 h electrolysis. Consequently, the GDEs were not particularly susceptible to cathodic corrosion at the applied electrolysis conditions. They were most stable in contact with electrolyte (B), followed by electrolyte (A) and then electrolyte (C). As all catholyte's Sn^{2+} concentrations were relatively low, no negative effects on the microbial PHB synthesis were expected for any of them. Details on ICP-OES analysis as well as before and after scanning electron microscope (SEM) images of all GDEs are supplied in the SI (Section 1.6 and 3.3).

IC analysis revealed that initial and final PO_4^{3-} concentrations after electrolysis differed only slightly in all experiments (SI, Section 1.7). In contrast to PO_4^{3-}, the final concentrations of Na^+ and/or K^+ increased compared to their initial concentrations for all three electrolytes. At the same time, the concentrations in the respective anolytes decreased accordingly (SI, section 1.7). Nearly all alkali cations from both catholyte and anolyte are found in the catholyte after electrolysis. Therefore, their concentrations should have nearly doubled in the catholyte. However, the catholytes increased in volume during electrolysis due to osmosis. This results in concentrations slightly below doubling, whereas the total molar amounts were constant. All IC analysis results are provided in the SI (Section 1.7).

Although an increase of final cation concentrations was induced by electrolysis, the catholytes could still serve as e-formate feed in a fed-batch reactor system, as these higher concentrations do not alter the main incubation's cation concentration significantly at herein examined feeding times.

Microbial PHB synthesis with *C. necator*

The three phosphate buffers were also investigated for microbial PHB synthesis with *C. necator*. Additionally, it was deduced from previous results[25] that a formate concentration below 100 mmol L^{-1} could be advantageous for PHB synthesis. Consequently, PHB synthesis was carried out with the three respective phosphate buffers at different formate concentrations in a range from 0 to 100 mmol L^{-1}. The aim was to identify the most suitable buffer composition alongside the formate concentration that should be maintained for PHB synthesis in bioreactors with a semi-automated e-formate feed. Hence, preliminary incubations for PHB synthesis were designed accordingly.

All incubations were conducted with *C. necator* (wildtype) resting cells. The resting cells were acquired by raising *C. necator* cells from cryo stock in a first preculture in Lysogeny broth (LB), followed by a second preculture in formate-based minimal medium. The bioconversion of formate to PHB was carried out in shake flasks for 4 h. The target value of the initial OD_{600} was 0.2, which was intentionally low to prevent large changes in formate concentration during incubation as formate is consumed for PHB synthesis. The real OD_{600} after the inoculation was measured and differed slightly, therefore the results were normalised to the actual initial OD_{600}. Figure 3 compares the achieved PHB concentrations as well as the amount of PHB per consumed formate for all three phosphate buffers and the respective formate concentrations.

Each incubation series was performed in triplets ($n = 3$) and 0 mmol L^{-1} formate was examined to ensure the determined PHB content was synthesised on formate. The resting cells already contained PHB from pre-cultivation, which was subtracted from all incubation data. For some incubations, especially with 0 mmol L^{-1}, negative PHB concentrations were observed, since the cells could neither synthesise new PHB nor had they formate to sustain their energy demand, so the PHB originating from pre-cultivation was consumed instead.

Besides, the results show that the highest PHB concentration occurred at different initial formate concentrations for each phosphate buffer. This is also true for the highest amount of PHB per consumed formate. Generally, the highest PHB

Table 1. Comparison of cation concentrations in the catholyte before and after formate electrosynthesis (22 h, 150 mA cm^{-2}) for three phosphate buffers as electrolytes: (A) 0.2 M KH_2PO_4/K_2HPO_4, (B) 0.2 M NaH_2PO_4/K_2HPO_4 and (C) 0.2 M NaH_2PO_4/Na_2HPO_4. Sn^{2+} concentration was quantified via ICP-OES, Na^+ and K^+ concentrations via IC.

Buffer	$c(Na^+)^{[a]}$/mmol L^{-1}	$c(K^+)^{[a]}$/mmol L^{-1}	$c(Na^+)^{[b]}$/mmol L^{-1}	$c(K^+)^{[b]}$/mmol L^{-1}	$c(Sn^{2+})^{[b]}$/μmol L^{-1}
A ($n = 3$)	3.0[c]	289.3[c]	5.5 ± 0.3	535 ± 2	11 ± 3
B ($n = 6$)	102.2[c]	192.1[c]	187 ± 1	355 ± 3	8.7 ± 1.6
C ($n = 3$)	297.2[c]	1.4[c]	536 ± 2	2.5 ± 0.6	20 ± 6

[a] Before electrolysis. [b] After electrolysis. [c] Measured $n = 1$.

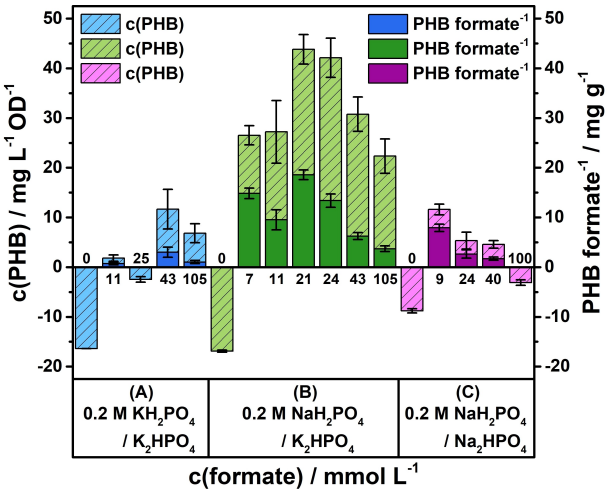

Figure 3. Comparison of PHB concentration normalised to initial OD_{600} (column, line pattern) and PHB per formate (column, solid) during PHB synthesis with *C. necator* resting cells in shake flasks with variable initial formate concentrations specified at the columns in different phosphate buffers: (A) 0.2 M KH_2PO_4/K_2HPO_4 (blue), (B) 0.2 M NaH_2PO_4/K_2HPO_4 (green), (C) 0.2 M NaH_2PO_4/Na_2HPO_4 (purple). Incubation conditions ($n=3$), Initial $OD_{600} \approx 0.2$, V = 75 mL, Duration = 4 h, T = 30 °C, Shaking = 180 rpm.

concentration coincided with the highest amount of PHB per formate for all three buffer compositions. To optimise formate conversion to PHB and thereby process efficiency, the amount of PHB per consumed formate was the main evaluation criterion.

In incubations with phosphate buffer (A), the highest achieved PHB concentration was 11.7 ± 4.0 mg L^{-1} OD^{-1} ($n=3$) with 3.0 ± 1.1 mg g^{-1} ($n=3$) PHB per formate at a starting formate concentration of 43 mmol L^{-1}. The corresponding average formate consumption rate was 21.5 ± 0.2 mmol L^{-1} h^{-1} OD^{-1} ($n=3$). In contrast, the best results in phosphate buffer (B) were obtained at 21 mmol L^{-1} formate. PHB concentration reached 43.8 ± 3.0 mg L^{-1} OD^{-1} ($n=3$) and 18.6 ± 1.0 mg g^{-1} ($n=3$) PHB per formate with an average formate consumption rate of 13.1 ± 0.2 mmol L^{-1} h^{-1} OD^{-1} ($n=3$). Finally, incubations in phosphate buffer (C) were best at 9 mmol L^{-1} formate. They reached 11.6 ± 1.1 mg L^{-1} OD^{-1} ($n=3$) PHB corresponding to 7.9 ± 0.8 mg g^{-1} ($n=3$) PHB per formate at an average formate consumption of 8.2 ± 0.2 mmol L^{-1} h^{-1} OD^{-1} ($n=3$).

The comparison of each buffer's best results revealed that the most efficient PHB synthesis had been achieved with buffer (B) regarding both the total PHB concentration and the amount of synthesised PHB per consumed formate. It follows that the presence of both Na^+ and K^+ is beneficial for PHB synthesis since neither solely Na^+ nor K^+ containing buffer allowed proper PHB synthesis. Although this was not the focus of this work and was not investigated further, it could be assumed that the absence of either K^+ or Na^+ might result in an overall decreased biological activity, possibly related to membrane potentials inside the cells. Besides the 1:2 ratio of Na^+/K^+ of buffer (B), the inverse Na^+/K^+ ratio of 2:1 has also been investigated but did not provide a higher PHB per formate ratio (SI, section 3.4). Consequently, the Na^+/K^+ ratio (1:2) of buffer (B) was preferred.

All in all, phosphate buffer (B) with 21 mmol L^{-1} formate was chosen for PHB synthesis in parallelised bioreactors with semi-automated e-formate feed. Thereby, 21 mmol L^{-1} formate has to be maintained within a relatively narrow window, as examined formate concentrations above and below (11 and 24 mmol L^{-1}) already have lower PHB to formate ratios. It is assumed that with increasing formate concentrations the substrate toxicity/stress caused by formate could play a role, which might lead to a decreased PHB to formate ratio. Nevertheless, compared to the starting point,[25] buffer adaption with lower formate concentration has improved PHB synthesis considerably.

Process Coupling

For the process coupling using phosphate buffer (B), six electrolyses were performed generating approximately 3 L of catholyte containing 441 mmol L^{-1} e-formate as feedstock. Afterwards, four incubations were carried out simultaneously in semi-automated bioreactors in the so called DASGIP® fermentation system. They were conducted with *C. necator* (wildtype) resting cells as before, which were obtained following the procedure described earlier. However, this time the second formate-based preculture was already grown on e-formate. Thus, the entire incubation process is based on formate originating from electrosynthesis.

The bioreactor incubations started with an initial OD_{600} of 1.80 in 340 mL of buffer (B) 0.2 M NaH_2PO_4/K_2HPO_4 containing 21 mmol L^{-1} e-formate. From then on, the cells were incubated for 7.5 h with hourly adapted e-formate feed rates from the stock solution to maintain 21 mmol L^{-1} e-formate. Samples for formate analysis by high-performance liquid chromatography (HPLC) were taken every 30 min for all bioreactors. However, only samples from two reactors every hour in the range of 0.5 h to 6.5 h of the incubation duration could be analysed instantly to adjust the catholyte feed at every full hour to maintain a constant formate concentration. Samples for PHB analysis were taken every two hours and at the incubation's end for all reactors, respectively. All changes in volume caused by sampling and e-formate feed were considered for result calculations, especially for normalising all results to the initial OD_{600}. Figure 4 relates e-formate concentration and its consumption to PHB synthesis during the incubation process.

Section 1 of Figure 4 shows that the e-formate concentration deviated significantly from the target e-formate concentration of 21 mmol L^{-1} throughout incubation. This was caused by the only available formate quantification method, samples had to be analysed off-line via HPLC and a single measurement took 25 min. Therefore, the hourly e-formate feed had to be extrapolated based on the e-formate consumption rate determined within the first half of each feeding interval. Nonetheless, the microorganisms always had e-formate to feed on as its concentration never fell to zero. Despite the variation in concentration, e-formate was consumed continuously with an average consumption rate of 10.2 ± 2.3 mmol L^{-1} h^{-1} OD^{-1} ($n=$

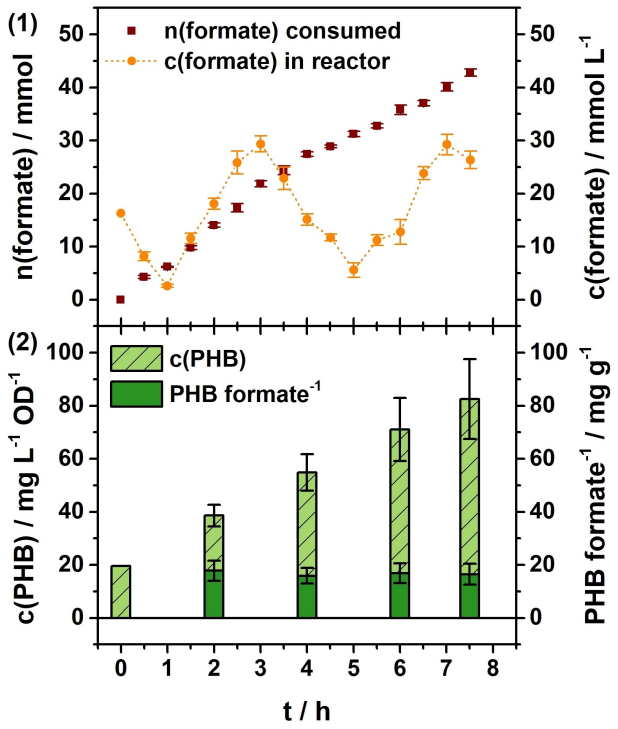

Figure 4. PHB synthesis of *C. necator* resting cells in semi-automated bioreactors with e-formate stock solution feed ($n=4$). (1) Consumed formate and formate concentration within the reactor during incubation. (2) PHB concentration normalised to initial OD_{600} (column, light green, line pattern) and continuous PHB formate^{-1} (column, green, solid). Incubation conditions ($n=4$): Medium = 0.2 M NaH_2PO_4/K_2HPO_4 (equimolar), Initial $OD_{600}=1.80$, Initial V = 340 mL, T = 30 °C, c(e-formate) of feed = 441 mmol L^{-1}, Initial e-formate feed = 6.9 mL h^{-1} (adjusted during runtime), Runtime = 7.5 h.

4). Thereby, the highest observed consumption rate was 13.1 ± 0.9 mmol L^{-1} h^{-1} OD^{-1} ($n=4$) in the third hour.

Equally important, PHB concentration increased continuously as well and reached 83 ± 16 mg L^{-1} OD^{-1} (≙ 110 ± 20 mg L^{-1}, $n=4$) at the end of incubation (Figure 4, Section 2). Considering that the cells already contained PHB from pre-cultivation, 63 ± 16 mg L^{-1} OD^{-1} ($n=4$) PHB were synthesised during bioreactor incubation with an average PHB synthesis rate of 8.4 ± 2.1 mg L^{-1} OD^{-1} h^{-1} ($n=4$). This corresponds to a final overall PHB per formate ratio of 16.5 ± 4.0 mg g^{-1} ($n=4$). Moreover, this ratio was also relatively constant throughout incubation despite the changes in e-formate concentration.

Compared to the shake flask incubation, the incubation results of the bioreactors were different. Their average formate consumption rate was 10.2 ± 2.3 mmol L^{-1} h^{-1} OD^{-1} ($n=4$), which was lower than the 13.1 ± 0.2 mmol L^{-1} h^{-1} OD^{-1} ($n=3$) in the shake flasks. Nevertheless, a similar consumption rate of 13.1 ± 0.9 mmol L^{-1} h^{-1} OD^{-1} ($n=4$) was reached in the third hour. Apart from that, the final PHB concentration obtained in the bioreactors of 63 ± 16 mg L^{-1} OD^{-1} ($n=4$) was higher compared to 43.8 ± 3.0 mg L^{-1} OD^{-1} ($n=3$) in the shake flasks. However, this is most probably due to the longer incubation time (7.5 h instead of 4 h) and a higher formate availability. Furthermore, the PHB amount per formate shows that PHB synthesis was marginally more efficient in shake flasks. These incubations resulted in 18.6 ± 1.0 mg g^{-1} ($n=3$) PHB per formate whereas the bioreactors yielded 16.5 ± 4.0 mg g^{-1} ($n=4$). This was mainly attributed to the challenging adjustment of the e-formate feed described above, as the target e-formate concentration could not be maintained throughout the complete incubation. The shake flask results for formate concentrations above and below 21 mmol L^{-1} support this hypothesis further, as they showed a lower PHB to formate ratio. Even though PHB synthesis was marginally more efficient in shake flasks, it was successfully transferred to the semi-automated, parallel fermenter system. Furthermore, the initial OD_{600} was increased approximately by factor 10 while reaching a similar PHB per formate ratio, which is crucial for the space-time yield of the process. All discussed deviations were mainly attributed to limitations of the e-formate feed control, which could be addressed by establishing an alternative, on-line formate analysis method in the future. All in all, transfer and scale-up of the microbial PHB synthesis were successfully demonstrated.

In the predecessor study,[25] an average PHB synthesis rate of 3.2 mg L^{-1} OD^{-1} h^{-1} was obtained. Thus, a significant improvement to 8.4 ± 2.1 mg L^{-1} OD^{-1} h^{-1} ($n=4$) was achieved herein. Moreover, the PHB per formate ratio was increased to 16.5 ± 4.0 mg g^{-1} ($n=4$) in the bioreactors compared to 14.1 mg g^{-1} achieved in the shake flasks back then. Recently, Lim et al.[37] reported 11.5 mg h^{-1} as highest PHB synthesis rate on e-formate at the time. Normalised to their starting OD_{600} (0.9) and initial incubation volume (2 L), this equals a PHB synthesis rate of 6.4 mg L^{-1} OD^{-1} h^{-1}, which is below the rate achieved herein now. Given the difference in incubation time and conditions, these rates have limited comparability though.

Process Balancing

The overarching aim of this study was to demonstrate the excell coupling of the subprocesses *eCO$_2$RR* to formate and PHB biosynthesis as well as to use the process data to conduct a transparent process balancing and evaluation under current and realistic assumptions. The authors would like to encourage others to do the same alongside an analysis under predicted future conditions, as it is currently underrepresented and could help draw attention to the main realisation barriers.

Hence, after demonstrating the coupling of formate electrosynthesis to microbial PHB synthesis on a larger and semi-automated lab scale, the resulting overall process was evaluated. For this purpose, the overall process yield was calculated based on the yields of both subprocesses. The yield of formate electrosynthesis (first subprocess) is equivalent to the formate FE discussed earlier. All electrolyses carried out for e-formate feedstock production resulted in a formate FE of 76.6 ± 1.4 % ($n=6$). To calculate the microbial PHB synthesis yield (second subprocess), a theoretical PHB yield based on the microorganism's metabolism was determined. Referring to Vlaeminck et al.,[39] *C. necator* uses 33 equivalents formic acid/formate to synthesise a single equivalent PHB monomer unit. Based on this stoichiometric ratio, a PHB yield of 29.1 ± 7.1 % ($n=4$) was obtained in the bioreactors. Thus, an overall process yield of

$22.3 \pm 5.5\,\%$ was achieved. All equations for yield calculations are provided in the Experimental Section.

For comparison with the initial coupled process,[25] PHB and overall process yield were calculated from the aforementioned study in the same manner because previously only an overall FE (4%) had been considered. Consequently, $49.7 \pm 0.9\,\%$ formate FE and 24.1% PHB yield resulted in an overall process yield of 12%. This shows that the overall process yield has been nearly doubled herein, especially due to the improved formate FE. In contrast, the current PHB yield is only about five percent higher than the former and still relatively low. Therefore, the main opportunity for further optimisation lies within the PHB synthesis. On the one hand, the PHB yield could potentially be optimised by lowering the salt/phosphate load, which is currently a compromise between the *eCO$_2$RR* and the PHB synthesis. On the other hand, more fundamental approaches such as evolutionary engineering, as it has been shown for *C. necator* and formate,[40] or genetic metabolism optimisation[41] would most likely increase the PHB yield. The need for an optimisation in this sense becomes even clearer if one takes economic aspects into account. Figure 1 (Section 2) contains an energy cost assessment for the overall process with PHB as final product alongside key process data.

Formate electrosynthesis from CO_2 required 10.3 ± 0.5 kWh kg^{-1} of electric energy. According to the Federal Statistical Office of Germany, 0.182 € kWh^{-1} were the average electricity costs for non-households in the first half of 2023 (excluding taxes, fees, levies and charges).[35] Consequently, electrosynthesised formate would cost 1.88 ± 0.08 € kg^{-1}, which is higher than exemplary market prices for formic acid of 0.37 € kg^{-1} and 0.69 € kg^{-1} (0.40 $ kg^{-1}[42] and 0.74 $ kg^{-1},[43] respectively with 1 € ≙ 1.08 $). With the achieved PHB per formate ratio, the final cost for PHB from CO_2 would amount to 114 ± 19 € kg^{-1}. Even with a quantitative PHB yield according to *C. necator's* metabolism,[39] PHB cost would be 34 € kg^{-1} based on the electric energy costs mentioned above, which is currently far off an economic price range.

In regard of this data, lowering the average terminal voltage required for formate electrosynthesis has great potential to lower overall energy costs. This could be achieved by flow reactor optimisation, for example by integration of a membrane assembled anode. However, the main cause increasing final PHB energy costs is the inefficient formate conversion pathway[39] of *C. necator*. This microorganism was chosen for this study as it remains a robust and reliable model system for demonstrating the coupling of formate electrosynthesis from CO_2 to microbial PHB synthesis. Nonetheless, either *C. necator* needs to be optimised, as has been reported by Claassens et al.[41] by replacing the rather inefficient Calvin cycle with the reductive glycine pathway, or *C. necator* needs to get substituted with a production strain harbouring a more efficient metabolism to move towards realisation of the demonstrated coupling on larger scale.

Conclusions

In this study, the *eCO$_2$RR* to formate has been coupled to microbial PHB synthesis in parallelised bioreactors with a semi-automated formate feed without intermediate downstream feed purification or concentrating. Beforehand, three biocompatible phosphate-based buffers were examined as both electrolytes and incubation buffers, with 0.2 M NaH_2PO_4/K_2HPO_4 allowing the most efficient coupling.

The formate feedstock solution was generated as catholyte by electrochemical CO_2 reduction at GDE. The GDE incorporated relatively inexpensive Sn (approx. 95 € kg^{-1}) as electrocatalyst and were self-fabricated by a fast, easy, reproducible and scalable fabrication method. They were reliably operated at 150 mA cm^{-2} for 22 h and no significant cathodic corrosion was observed. The catholyte used as feed contained 441 ± 9 mmol L^{-1} ($n = 6$) formate, which corresponded to an overall formate FE of $76.6 \pm 1.4\,\%$ ($n = 6$).

The subsequent PHB synthesis was carried out with *C. necator* (wildtype), based on preliminary experiments evaluating the ideal formate concentration with regards to maximum PHB production and highest PHB per formate ratio in semi-automated bioreactors. Despite challenging formate feed adjustment during incubation, 63 ± 16 mg L^{-1} OD^{-1} ($n = 4$) PHB was reached. This corresponds to an average PHB synthesis rate of 8.4 ± 2.1 mg L^{-1} OD^{-1} h^{-1}, which is among the highest reported in literature so far to the best of the authors' knowledge. According to *C. necator's* metabolism,[39] a PHB yield of $29.1 \pm 7.1\,\%$ ($n = 4$) was obtained. Consequently, the coupling of both subprocesses resulted in a considerably improved overall process yield of $22.3 \pm 5.5\,\%$.

Finally, energy costs of the demonstrated overall process were assessed for formate (1.88 ± 0.08 € kg^{-1}) and PHB (114 ± 19 € kg^{-1}) under current and realistic assumptions (0.182 € kWh^{-1}[35]). The assessment revealed that although the concept is promising, its realisation depends on further development of both subprocesses as well as the availability of inexpensive, renewable energy in the future.[44]

Experimental Section

Gas Diffusion Electrodes

The gas diffusion electrodes (GDE) were fabricated by pressing a Sn based catalyst mixture onto Ni foam as support material and current collector with a heating press. The catalyst mixture (30.00 g) consisted of Sn (87.5 wt%, 26.25 g, particle size ≤ 20 µm, Metallpulver24, Sankt Augustin, Germany) and polytetrafluoroethylene (PTFE) powder (12.5 wt%, 3.75 g, Dyneon™ PTFE TF 2072Z, 3M, Saint Paul, USA). The catalyst mixture was homogenised in a knife mill, the mixing (30 s, 25000 rpm) lead to a temperature increase of the mixture ($T > 35\,°C$). After cooling to room temperature (RT), the catalyst mixture (4.00 g) was equally distributed onto Ni foam ($d = 1.4$ cm, 3.5 cm×4.0 cm ≙ 14 cm^2, Ni-5763, density 420–450 g m^{-2}, Recemat BV, Dodewaard, Netherlands) with a sieve and a stencil (Cut-out 3.5 cm×4.0 cm). The GDE blank was placed in between two pieces of ordinary baking sheet in the heating press and compressed (plate temperature 120 °C, pressure 10 bar, duration

60 s). After compressing, any excess material was removed. The GDE's catalyst loading *b* was determined by differential weighing and its thickness *d* was measured at the centre point. GDE photographs are provided in the SI (Section 3.2)

Electrolysis flow reactor set-up

The electrochemical reduction of CO_2 to formate was performed in a custom designed, gas-fed flow reactor (Figure 5). It consisted of three different compartments made from PEEK (polyetheretherketone), one for gaseous CO_2, followed by a catholyte and an anolyte compartment, respectively. The CO_2 compartment (2.0 cm×2.5 cm×1 mm, flow field) was separated from the catholyte compartment by the GDE (3.5 cm×4.0 cm, accessible geometrical surface area 2.0 cm×2.5 cm ≙ 5 cm^2). The GDE was placed in between two silicone gaskets (thickness 0.5 cm) to prevent fluid leakage and enable application of CO_2 overpressure. The following catholyte compartment frame (thickness 3 mm) had spatial cut-outs to allow equal distribution of catholyte flow and a port to incorporate a reversible hydrogen electrode (RHE, Mini HydroFlex, Gaskatel GmbH, Kassel, Germany) as reference electrode. Catholyte and anolyte compartment were separated by a proton exchange membrane (2.5 cm×3.0 cm, Nafion™, PFSA 117, DuPont, Wilmington, USA) sealed in between two silicone gaskets (thickness 0.5 cm). The anolyte compartment (2.0 cm×2.5 cm×2.0 cm) had spatial cut-outs like the catholyte compartment and contained a titanium mesh coated with Ir mixed oxide as an anode (PLATINODE® EP, 2.0 cm×2.5 cm, mesh type F, anode type 177, Umicore, Brussels, Belgium). The assembled reactor was enclosed in between two steel plates (d = 8 mm) to ensure an equal distribution of compacting pressure.

The CO_2 was fed into the reactor through a water-filled bubble counter to saturate the CO_2 with water at RT. It flowed top-down through the gas compartment to prevent fluid accumulation within.

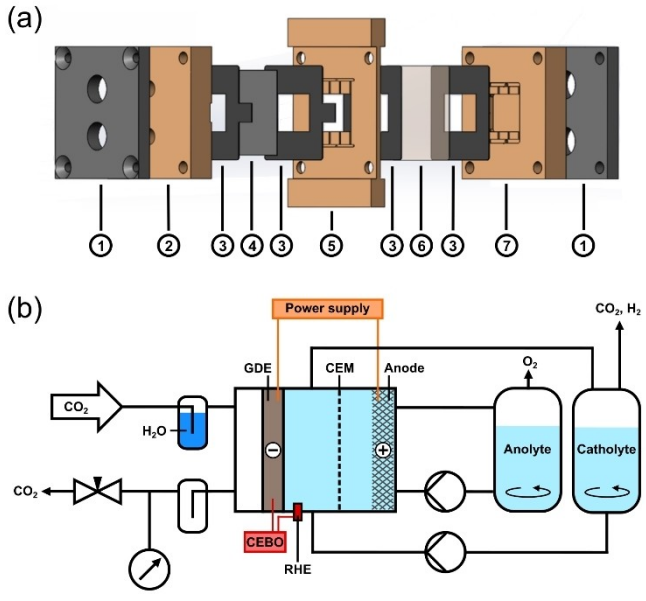

Figure 5. (a) Schematic illustration of the custom designed, gas-fed flow reactor fabricated by the DECHEMA workshop composed of: (1) Stainless-steel plate, (2) CO_2 compartment with flow-field, (3) silicone gasket, (4) GDE (5 cm^2 geometrically accessible), (5) catholyte compartment with a reversible hydrogen electrode (RHE) port, (6) cation exchange membrane (CEM), (7) anolyte compartment (incorporating the anode). (b) Schematic set-up for the operation of the electrolysis flow reactor for the electrosynthesis of formate with gaseous CO_2 as starting material (CEBO = Data logger).

The CO_2 outlet of the reactor's gas compartment was followed by a collecting vessel (500 mL) to collect any electrolyte potentially breaking through the GDE. The CO_2 overpressure was adjusted at the end of the CO_2 line with a regulating valve as well a differential pressure sensor combined with a pressure meter.

Catholyte and anolyte were circulated between the respective reactor compartments and reservoir with a peristaltic pump. To prevent gas entrapment and maintain fluid coverage of the electrodes, both anolyte and catholyte were passed through the reactor bottom-up. Further details can be found in the SI (Section 1.3).

Formate electrosynthesis

All electrosyntheses were performed for 22 h. A power supply unit (NGP804, Rohde & Schwarz GmbH & Co. KG, Munich, Germany) was employed to run the electrolysis, it recorded terminal voltage, current and power. Furthermore, the electrode potential of the GDE was referenced to RHE and recorded. The electrosynthesis started with a current ramp in the first hour, in which the current density was increased in steps of 12.5 mA cm^{-2} every 5 min until it reached 150 mA cm^{-2} (750 mA in total), which was kept constant for the remaining 21 h runtime.

CO_2 was supplied to the GDE in the gas compartment at a flow rate of 15–20 mL min^{-1} and an initial overpressure of approx. 100 mbar relative to ambient pressure. The pressure was recorded continuously during the running electrolysis. Gas samples were collected in the last hour of the electrolysis (t = 21 h) at the exhaust of the catholyte reservoir, where gas mainly bubbled through (approx. 50 mL in 5 min) and analysed by gas chromatography (SI, section 1.8).

Three different phosphate-based buffers were used as electrolyte: (A) 0.2 M KH_2PO_4/K_2HPO_4, (B) 0.2 M NaH_2PO_4/K_2HPO_4 and (C) 0.2 M NaH_2PO_4/Na_2HPO_4 (equimolar, respectively), with pH values of 6.67 ± 0.05 (A, n = 3), 6.61 ± 0.05 (B n = 6) and 6.53 ± 0.05 (C, n = 3). For each electrolysis, anolyte and catholyte had a starting volume of 500 mL (volumetric flask, ISO 1042). Anolyte and catholyte were circulated continuously at a flow rate of 40 mL min^{-1} between flow reactor compartment and reservoir, respectively. During the electrolysis, catholyte samples (1 mL) were taken hourly in the first six (t = 0–6 h) and the last four (t = 19–22 h) hours to monitor pH value, formate concentration and calculate the corresponding FE. After electrolysis, the respective anolyte and catholyte volume was determined by its weight and density. Therefore, the density was calculated by taking samples (1 mL) and weighing them (n = 3). Catholyte containing electrochemically generated formate (e-formate) was stored at −20 °C until its application for microbial PHB synthesis. The GDE was rinsed with H_2O and dried at RT. Further details can be found in the SI (section 1.4).

Sn quantification by inductively coupled plasma optical emission spectrometry (ICP-OES)

ICP-OES measurements were performed in radial viewing mode on Agilent 5800 ICP-OES equipped with an SPS 4 Autosampler, a borosilicate double-pass spray chamber and a Seaspray concentric glass nebulizer.

The wavelength for Sn determination was 283.998 nm and the Ar wavelength 420.067 nm served as an internal standard, for which errors less than 5% were accepted. All electrolyte samples had to be diluted by factor 4 to meet the internal standard criterion. The catholyte's Sn content was quantified via standard addition of a stock solution containing 1 ppm Sn. The stock solution was

prepared from a Sn standard (1000 ppm, Single-Element ICP-Standard-Solution, Lot N. 83131639, Carl Roth GmbH + Co. KG) via a dilution series by factor 10 using volumetric flasks (100 mL, ISO 1042).

For each sample, four different aliquots of stock solution (0.5, 1.0, 1.5, 2 mL) were added to the undiluted sample (1 mL). The analyte spiked samples were filled up to 4 mL with H_2O, respectively. Hence, five points were measured for each sample. Linear fits with $R^2 \geq 0.995$ were accepted due to the limited available sample volumes and several signals being close to the lower limit of detection (LOD, approx. 0.2 ppm for Sn at 283.998 nm) resulting out of the necessary dilution factor.

Cation analysis by ion chromatography (IC)

IC measurements to determine cation concentrations were performed on Dionex™ ICS-5000$^+$ DC (Pre column = Dionex™ IonPac CG17, Column = Dionex™ IonPacTM CS17, Analytical 2×250 mm, Suppressor = CERS 500, 2 mm). Methanesulphonic acid (MSA) served as eluent with a gradient method (steps 1–4: 1. −5–0 min, 1.5 mmol L^{-1} MSA (preparation step), 2. 0–25 min, 1.5–2.1 mmol L^{-1} MSA, 3. 25–40 min, 6 mmol L^{-1} MSA, 4. 40–60 min, 1.5 mmol L^{-1} MSA) at 0.1 mL min^{-1} flow rate. Samples were diluted by factor 200 or 400, Na^+ (retention time = 29.1 min) and K^+ (retention time = 35.1 min) were detected with a conductivity cell.

Standards to determine the concentrations of Na^+ and K^+ were prepared by a dilution series of a stock solution. The stock solution was prepared with NaCl (3.254 g ≙ 1280 ppm Na^+) and KCl (2.441 g ≙ 1280 ppm K^+) in a volumetric flask (1 L, ISO 1042). All combined standards (1, 2, 4, 8, 16, 32, 64 ppm) were measured (n = 1) and their signal areas fitted (R^2 = 0.9999, linear fit forced through zero).

Formate quantification by high-performance liquid chromatography (HPLC)

Formate concentration in both electrolysis and incubation samples were determined via HPLC (LC-20AD, SIL-20AC HT, CBM-20 A, CTO-20AC, SPD-M20A – Shimadzu, Kyoto, Japan). Samples from incubations were centrifuged (14100×g, 5 min) prior to analysis to remove all cells.

The HPLC unit was equipped with a Rezex ROA – Organic Acid (8%) column (300 mm×7.8 mm, Phenomenex, California, USA) and the following method parameters were employed: 5 mmol L^{-1} H_2SO_4, 0.6 mL min^{-1}, 30 °C, 30 ± 1 bar, photodiode array detector (λ = 194 nm), 15.3 min (retention time), 25 min (duration).

Formate standards were prepared by a dilution series from a stock solution. The stock solution was prepared with HCOONa (3.482 g, 51.2 mmol) in a volumetric flask (100 mL, ISO 1042). All formate standards (8, 16, 32, 64, 128, 256, 512 mmol L^{-1}) were measured (n = 3) and their signal areas fitted linearly (R^2 = 0.9999, fit forced through zero).

PHB quantification by high-performance liquid chromatography (HPLC)

PHB was depolymerised to its monomer unit crotonic acid for quantitative analysis. Sample preparation was conducted as follows: Samples were taken from the cultivation broth (10 or 30 mL, depending on the available volume). They were centrifuged (6000×g, 30 min) and the supernatant was discarded. The cell pellet was resuspended in 1 mL H_2O. The resulting cell suspension was transferred into a 2 mL centrifuge tube and centrifuged (14100×g, 5 min). The supernatant was discarded, and the cell pellet was dried overnight (100 °C). The dried cell pellet was mixed with 1 mL of concentrated H_2SO_4 and incubated (99 °C, 500 rpm, 60 min). The resulting solution was diluted 1:50 with H_2O and subsequently used for HPLC analysis.

It was performed on an HPLC-Unit (LC-20AD, SIL-20AC HT, CBM-20 A, CTO-20AC, SPD–M20 A – Shimadzu, Kyoto, Japan) equipped with the Rezex ROA – Organic Acid (8%) column (300 mm ×7.8 mm, Phenomenex, California, USA). Crotonic acid was analysed with the following method parameters: 5 mmol L^{-1} H_2SO_4, 0.6 mL min^{-1}, 40 °C, 27 ± 1 bar, photodiode array detector (λ = 207 nm), 29.2 min (retention time), 40 min (duration).

PHB standards were prepared by a dilution series from a stock solution. For preparation of the stock solution, PHB (7.45 mg) was weighed in a 2 mL centrifuge tube. The PHB was depolymerised in the same manner as described for the dried cell pellets above. Hence, the PHB was mixed with 1 mL of concentrated H_2SO_4, incubated (99 °C, 500 rpm, 60 min) and afterwards diluted 1:50 with H_2O. All PHB standards (25, 50, 100, 250, 500, 1000 µg) were measured (n = 3) and their signal areas fitted linearly (R^2 = 0.9997, fit forced through zero).

Microorganisms

The bioconversion of either commercial or electrosynthesised formate (e-formate) was demonstrated with *Cupriavidus necator* wildtype (DSM-428, DSMZ, Braunschweig, Germany), which produces PHB from formate under NH_4^+ limitation.

Growth media

The cultivation and incubation of *C. necator* was carried out with the different growth media following below.

Lysogeny broth (LB): Yeast extract (5 g L^{-1}), tryptone (10 g L^{-1}) and NaCl (5 g L^{-1}) in deionized water, the pH was set to 7.0 with NaOH (2 M) and HCl (2 M).

Minimal medium with commercially available formate: HCOONa (6.801 g L^{-1}), Na_2HPO_4 (2.895 g L^{-1}), $NaH_2PO_4 \cdot 2\ H_2O$ (3.980 g L^{-1}), K_2SO_4 (0.171 g L^{-1}), $MgSO_4 \cdot H_2O$ (0.390 g L^{-1}), $(NH_4)_2SO_4$ (0.980 g L^{-1}), $CaSO_4 \cdot 2\ H_2O$ (0.097 g L^{-1}) and trace element solution (350 µL L^{-1}). All media components were prepared sterile as separate stock solutions and combined prior to each experiment. The pH value was set to 7.0 with sterile H_2SO_4 (2 M) and NaOH (2 M).

Trace element solution: $FeSO_4 \cdot 7\ H_2O$ (15.00 g L^{-1}), $MnSO_4 \cdot H_2O$ (1.46 g L^{-1}), $ZnSO_4 \cdot 7\ H_2O$ (2.40 g L^{-1}), $CuSO_4 \cdot 5\ H_2O$ (0.48 g L^{-1}), $Na_2MoO_4 \cdot 2\ H_2O$ (1.80 g L^{-1}), $NiSO_4 \cdot 6\ H_2O$ (1.50 g L^{-1}), $CoSO_4 \cdot 7\ H_2O$ (0.04 g L^{-1}) dissolved in 0.1 M HCl.

Minimal medium with e–formate: The calculated volume of the catholyte (depending on the e-formate concentration) for 100 mmol L^{-1} e-formate was mixed with the ingredients of the minimal medium described above, except for HCOONa, Na_2HPO_4 and NaH_2PO_4, which were not added in this case.

Formate-containing buffer for resting cells: The phosphate buffer was either (A) 0.2 M KH_2PO_4/K_2HPO_4, (B) 0.2 M NaH_2PO_4/K_2HPO_4 or (C) 0.2 M NaH_2PO_4/Na_2HPO_4. The different formate concentrations were adjusted with either commercially available formate (HCOONa or HCOOK) or e-formate feedstock originating from electrosynthesis.

Cultivation and incubation of *C. necator*

All experiments were conducted using a first preculture raised in LB and a second preculture raised in minimal medium before the main incubation in formate-containing buffer. All incubations were carried out at 30 °C. All shake flask and test tube incubations were shaken at 180 rpm (shaking diameter of 25 mm). The second precultures (in minimal medium) were conducted in shake flasks of varying sizes depending on the required volume for the main incubation with filling volumes of 25% of the nominal volume. All samples taken during the incubation were frozen at −20 °C until further analysis.

One or several *C. necator* precultures (depending on the required volume for further cultivation steps) were raised from a cryo stock in 5 mL LB in test tubes. After 22–24 h of incubation, cells were harvested by centrifugation (5 min, 5000×g), washed with fresh minimal medium, centrifuged again (5 min, 5000×g), resuspended and added to the required volume of prepared minimal medium to reach a starting OD_{600} of 0.05. After 24 h the second precultures were harvested by centrifugation (7 min, 5000×g), washed with fresh sterilised buffer, centrifuged again (7 min, 5000×g) and used for inoculation of the main incubation of resting cells in formate-containing buffer.

Incubation in shake flasks: Incubation of resting cells in buffer (A) 0.2 M KH_2PO_4/K_2HPO_4, (B) 0.2 M NaH_2PO_4/K_2HPO_4 or (C) 0.2 M NaH_2PO_4/Na_2HPO_4 with different formate concentrations were performed in 300 mL shaking flasks with a filling volume of 75 mL. Main cultures were inoculated with the calculated cell amount for an initial OD_{600} of 0.2, whereby the actual initial OD_{600} could slightly deviate. All incubation conditions were run in triplicates.

Incubation in semi-automated parallelised bioreactors: Main incubations of resting cells in semi-automated bioreactors were performed in the DASGIP® Parallel Bioreactor System (DASGIP AG, Jülich, Germany, Modules: Gas supply system = MX4/4, Temperature control system/Speed control system = TC4/SC4, Multipump module = MP8, Sensor amplifier = PH4PO4, DO-Sensor = InPro6820/12/220 from Mettler Toledo, pH electrode = 405-DPAS-SC-K8 S/225 from Mettler Toledo, PTFE air filter = Midisart® 2000 from Sartorius) in quadruplets. The initial incubation volume was 340 mL of buffer (B) 0.2 M NaH_2PO_4/K_2HPO_4, the initial OD_{600} was 1.80. The stirring frequency was set to 800 rpm, the pH value was measured and when reaching values above 7.2 regulated by automated adding of H_2SO_4 (1 M). All bioreactors were gassed with 6 sl min^{-1} compressed air. The initial feed of the catholyte containing 441 mmol L^{-1} e-formate was regulated to 6.9 mL h^{-1}. Samples (1 mL) for formate analysis by HPLC were taken every 30 min for all bioreactors. However, only samples of reactor 1 and 4 at 0.5 h, 1.5 h, 2.5 h, 3.5 h, 4.5 h, 5.5 h, 6.5 h of the incubation duration were analysed instantly to adjust the catholyte feed every full hour. At 0 h, 2 h, 4 h, 6 h and 7.5 h samples for PHB analysis were taken (10 mL).

Calculations

The FE for formate was calculated based on the determined amount of electrosynthesised formate using equation (1).

$$FE = \frac{F \cdot z \cdot n}{I \cdot t} \cdot 100\,\% \tag{1}$$

With FE = Faradaic efficiency of formate electrosynthesis/%, F = Faraday constant/A s mol^{-1}, z = Number of transferred electrons (z = 2), n = Amount of synthesised formate/mol, I = Current/A, t = Electrolysis runtime/s.

The results for each different phosphate-based electrolyte were averaged and their standard deviation was provided as uncertainty.

The PHB yield was calculated based on the determined amount of PHB using equation (2), (3) and (4).[39]

$$PHB\ yield = \frac{m(PHB)}{m(PHB,\ theo)} \cdot 100\,\% \tag{2}$$

With $PHB\ Yield$ = Yield of the microbial PHB synthesis based on e-formate, $m(PHB)$ = Mass of synthesised PHB/mg, $m(PHB,\ theo)$ = Theoretical mass of PHB at quantitative conversion of the consumed formate according to *C. necator's* metabolism[39]/mg.

$$m(PHB,\ theo) = M(CA) \cdot \frac{n(con.\ formate)}{33} \tag{3}$$

With $m(PHB,\ theo)$ = Theoretical mass of PHB at quantitative conversion of the consumed formate according to *C. necator's* metabolism[39]/mg, $M(CA)$ = 86.09 g mol^{-1} (crotonic acid), $n(con.\ formate)$ = Total amount of formate consumed in the bioreactor/mol.

$$33\ HCOOH + 12\ O_2 \rightarrow C_4H_6O_2 + 30\ H_2O + 29\ CO_2 \tag{4}$$

The results for each different bioreactor were averaged and their standard deviation was provided as uncertainty.

The overall process yield (OPY) was calculated based on the yields of the two subprocesses using equation (5) and (6).

$$OPY = FE \cdot PHB\ Yield \cdot 100\,\% \tag{5}$$

$$\Delta(OPY) = \sqrt{\begin{matrix}(PHB\ Yield)^2 \cdot (\Delta FE)^2 \\ +(FE)^2 \cdot (\Delta PHB\ Yield)^2\end{matrix}} \cdot 100\,\% \tag{6}$$

With OPY = Overall process yield, $\Delta(OPY)$ = Uncertainty of the overall process yield, FE = Faradaic efficiency of formate electrosynthesis/%, ΔFE = Standard deviation of the formate synthesis (n = 6)/%, $PHB\ Yield$ = Yield of the microbial PHB synthesis based on e-formate/%, $\Delta PHB\ Yield$ = Standard deviation of the PHB yield (n = 4)/%. All variables in equation (5) and (6) were divided by 100% prior to implementation for OPY and $\Delta(OPY)$ calculation.

Supporting Information

Supporting Information is available from the Wiley Online Library or from the corresponding author.

Acknowledgements

The authors are very grateful to the German Federal Ministry of Education and Research for their financial support (033RC031A and 033RC031B). Special thanks go to Dr. Nicky Bogolowski and Dr. Hans Joachim Kohnke (Gaskatel GmbH) for their support during GDE development. Furthermore, the authors would like to express their gratitude to Robin Kupec for his support in reactor design and to the DECHEMA Research Institute work-

shop, especially to Yvonne Hohmann, for construction of the custom electrolysis reactor. Finally, the authors would like to thank Jürgen Schuster and Jacqueline Patzsch for IC measurements as well as Alexander Langsdorf for sharing optimisations of the PHB analysis method. Open Access funding enabled and organized by Projekt DEAL.

Conflict of Interests

The authors declare no conflict of interest.

Data Availability Statement

The data that support the findings of this study are available in the supplementary material of this article.

Keywords: biosynthesis · CO_2 reduction · *Cupriavidus necator* · electrochemistry · polyhydroxybutyrate

[1] D. Pollok, S. R. Waldvogel, *Chem. Sci.* **2020**, *11*, 12386–12400.
[2] A. Wiebe, T. Gieshoff, S. Möhle, E. Rodrigo, M. Zirbes, S. R. Waldvogel, *Angew. Chem. Int. Ed.* **2018**, *57*, 5594–5619; *Angew. Chem.* **2018**, *130*, 5694–5721.
[3] S. Möhle, M. Zirbes, E. Rodrigo, T. Gieshoff, A. Wiebe, S. R. Waldvogel, *Angew. Chem. Int. Ed.* **2018**, *57*, 6018–6041; *Angew. Chem.* **2018**, *130*, 6124–6149.
[4] M. G. Kibria, J. P. Edwards, C. M. Gabardo, C. Dinh, A. Seifitokaldani, D. Sinton, E. H. Sargent, *Adv. Mater.* **2019**, *31*, 1807166.
[5] S. A. Al-Tamreh, M. H. Ibrahim, M. H. El-Naas, J. Vaes, D. Pant, A. Benamor, A. Amhamed, *ChemElectroChem* **2021**, *8*, 3207–3220.
[6] T. Haas, R. Krause, R. Weber, M. Demler, G. Schmid, *Nat. Catal.* **2018**, *1*, 32–39.
[7] R. I. Masel, Z. Liu, H. Yang, J. J. Kaczur, D. Carrillo, S. Ren, D. Salvatore, C. P. Berlinguette, *Nat. Nanotechnol.* **2021**, *16*, 118–128.
[8] J. Jörissen, T. Turek, R. Weber, *Chem. Unserer Zeit* **2011**, *45*, 172–183.
[9] D. Kopljar, A. Inan, P. Vindayer, N. Wagner, E. Klemm, *J. Appl. Electrochem.* **2014**, *44*, 1107–1116.
[10] D. Kopljar, N. Wagner, E. Klemm, *Chem. Eng. Technol.* **2016**, *39*, 2042–2050.
[11] M. Stöckl, T. Lange, P. Izadi, S. Bolat, N. Teetz, F. Harnisch, D. Holtmann, *Biotechnol. Bioeng.* **2023**, *120*, 1465–1477.
[12] S. Malkhandi, B. S. Yeo, *Curr. Opin. Chem. Eng.* **2019**, *26*, 112–121.
[13] B. J. M. Etzold, U. Krewer, S. Thiele, A. Dreizler, E. Klemm, T. Turek, *Chem. Eng. J.* **2021**, *424*, 130501.
[14] Z. Liu, H. Yang, R. Kutz, R. I. Masel, *J. Electrochem. Soc.* **2018**, *165*, J3371–J3377.
[15] C.-T. Dinh, F. P. García De Arquer, D. Sinton, E. H. Sargent, *ACS Energy Lett.* **2018**, *3*, 2835–2840.
[16] R. B. Kutz, Q. Chen, H. Yang, S. D. Sajjad, Z. Liu, I. R. Masel, *Energy Technol.* **2017**, *5*, 929–936.
[17] A. Löwe, M. Schmidt, F. Bienen, D. Kopljar, N. Wagner, E. Klemm, *ACS Sustainable Chem. Eng.* **2021**, *9*, 4213–4223.
[18] X. Wang, S. Liu, H. Zhang, S. Zhang, G. Meng, Q. Liu, Z. Sun, J. Luo, X. Liu, *Chem. Commun.* **2022**, *58*, 7654–7657.
[19] H. Yang, J. J. Kaczur, S. D. Sajjad, R. I. Masel, *J. CO2 Util.* **2020**, *42*, 101349.
[20] H. Yang, J. J. Kaczur, S. D. Sajjad, R. I. Masel, *J. CO2 Util.* **2017**, *20*, 208–217.
[21] N. J. Claassens, C. A. R. Cotton, D. Kopljar, A. Bar-Even, *Nat. Catal.* **2019**, *2*, 437–447.
[22] O. Yishai, S. N. Lindner, J. Gonzalez De La Cruz, H. Tenenboim, A. Bar-Even, *Curr. Opin. Chem. Biol.* **2016**, *35*, 1–9.
[23] M. Stöckl, N. Claassens, S. Lindner, E. Klemm, D. Holtmann, *Curr. Opin. Biotechnol.* **2022**, *74*, 154–163.
[24] D. Jendrossek, D. Pfeiffer, *Environ. Microbiol.* **2014**, *16*, 2357–2373.
[25] M. Stöckl, S. Harms, I. Dinges, S. Dimitrova, D. Holtmann, *ChemSusChem* **2020**, *13*, 4086–4093.
[26] N. Teetz, D. Holtmann, F. Harnisch, M. Stöckl, *Angew. Chem. Int. Ed.* **2022**, *61*, e202210596.
[27] H. Li, P. H. Opgenorth, D. G. Wernick, S. Rogers, T.-Y. Wu, W. Higashide, P. Malati, Y.-X. Huo, K. M. Cho, J. C. Liao, *Science* **2012**, *335*, 1596–1596.
[28] L. Garrigues, L. Maignien, E. Lombard, J. Singh, S. E. Guillouet, *New Biotechnol.* **2020**, *56*, 16–20.
[29] J. Lu, C. J. Brigham, C. S. Gai, A. J. Sinskey, *Appl. Microbiol. Biotechnol.* **2012**, *96*, 283–297.
[30] J. S. Chen, B. Colón, B. Dusel, M. Ziesack, J. C. Way, J. P. Torella, *PeerJ* **2015**, *3*, e1468.
[31] M. Raberg, E. Volodina, K. Lin, A. Steinbüchel, *Crit. Rev. Biotechnol.* **2018**, *38*, 494–510.
[32] T. Krieg, A. Sydow, S. Faust, I. Huth, D. Holtmann, *Angew. Chem. Int. Ed.* **2018**, *57*, 1879–1882; *Angew. Chem.* **2018**, *130*, 1897–1900.
[33] S. Milker, D. Holtmann, *Microb. Cell Fact.* **2021**, *20*, 89.
[34] U. Schröder, F. Harnisch, L. T. Angenent, *Energy Environ. Sci.* **2015**, *8*, 513–519.
[35] "Electricity prices for non-household customers: Germany, half-years, annual consumption classes, price types," can be found under https://www-genesis.destatis.de/datenbank/beta/statistic/61243/table/61243-0005, **2023**, (accessed: 11.10.2023).
[36] A. Sydow, T. Krieg, R. Ulber, D. Holtmann, *Eng. Life Sci.* **2017**, *17*, 781–791.
[37] J. Lim, S. Y. Choi, J. W. Lee, S. Y. Lee, H. Lee, *Proc. Nat. Acad. Sci.* **2023**, *120*, e2221438120.
[38] T. Wirtanen, T. Prenzel, J.-P. Tessonnier, S. R. Waldvogel, *Chem. Rev.* **2021**, *121*, 10241–10270.
[39] E. Vlaeminck, K. Quataert, E. Uitterhaegen, K. De Winter, W. K. Soetaert, *J. Biotechnol.* **2022**, *343*, 102–109.
[40] C. H. Calvey, V. Sànchez I Nogué, A. M. White, C. M. Kneucker, S. P. Woodworth, H. M. Alt, C. A. Eckert, C. W. Johnson, *Metab. Eng.* **2023**, *75*, 78–90.
[41] N. J. Claassens, G. Bordanaba-Florit, C. A. R. Cotton, A. De Maria, M. Finger-Bou, L. Friedeheim, N. Giner-Laguarda, M. Munar-Palmer, W. Newell, G. Scarinci, J. Verbunt, S. T. De Vries, S. Yilmaz, A. Bar-Even, *Metab. Eng.* **2020**, *62*, 30–41.
[42] M. Solakidou, A. Gemenetzi, G. Koutsikou, M. Theodorakopoulos, Y. Deligiannakis, M. Louloudi, *Energies* **2023**, *16*, 1723.
[43] M. Jouny, W. Luc, F. Jiao, *Ind. Eng. Chem. Res.* **2018**, *57*, 2165–2177.
[44] J. Seidler, J. Strugatchi, T. Gärtner, S. R. Waldvogel, *MRS Energy Sustainability* **2020**, *7*, 42.

Manuscript received: November 21, 2023
Revised manuscript received: December 12, 2023
Accepted manuscript online: January 5, 2024
Version of record online: ■■, ■■

RESEARCH ARTICLE

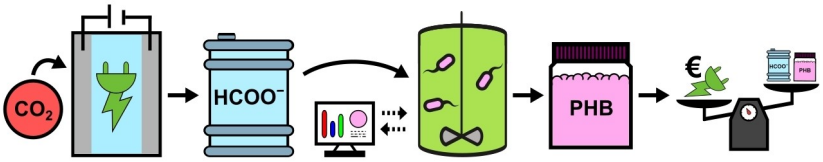

Formate electrosynthesis from gaseous CO_2 has been coupled to semi-automated, scalable microbial polyhydroxybutyrate (PHB) synthesis with *Cupriavidus necator*. CO_2 was converted at inexpensive Sn based gas diffusion electrodes. The generated catholyte served as feedstock for semi-automated *C. necator* feeding. For the combined processes, an overall process yield of $22.3 \pm 5.5\,\%$ was achieved.

*I. Dinges, I. Depentori, L. Gans, Prof. Dr. Ing. D. Holtmann, Prof. Dr. S. R. Waldvogel, Dr. M. Stöckl**